Sampling Sparse Multiband Signals with a Modulated Wideband Converter

Michael Lexa, Mike Davies and John Thompson
{michael.lexa,john.thompson,mike.davies}@ed.ac.uk

University of Edinburgh
Institute of Digital Communications
Technical Report

May 2010, Revised October 2010

Abstract

The modulated wideband converter (MWC) is a multi-channel uniform sub-Nyquist sampling strategy for acquiring continuous-time spectrally sparse signals. In this report, we present a concise mathematical description of the MWC that can be used as a reference for the accompanying MATLAB software that simulates the sampling and signal reconstruction. The derivations clarify system operation and give precise frequency and time domain descriptions.

1 Signal Model and System Description

Sparse multiband signals. A *multiband signal* $x(t)$ is a bandlimited, continuous-time, squared integrable signal that has all of its energy concentrated in one or more disjoint frequency bands (of positive Lebesque measure). Denoting the Fourier transform of $x(t)$ by $X(j\omega)$,

$$X(j\omega) = \int_{-\infty}^{\infty} x(t)\, e^{j\omega t}\, dt,$$

a bandlimited signal is one whose spectrum is bounded, i.e., $X(j\omega) = 0$ for $-\pi W \leq \omega < \pi W$ radians per second, for some positive real number W. Here, $W/2$ is the bandwidth of $x(t)$ and W is therefore the Nyquist frequency. The spectral support of a multiband signal is the union of the frequency intervals that contain the signal's energy. A *sparse* multiband signal is thus a multiband signal whose spectral support has Lebesgue measure that is small relative to the overall signal bandwidth [3]. If, for instance, all the active bands have equal bandwidth B Hz and the signal is composed of K disjoint frequency bands, then a sparse multiband signal is one satisfying $KB \ll W$.

Modulated wideband converter. The MWC is a multi-channel uniform sub-Nyquist sampling strategy for acquiring sparse multiband signals [1]. Each of the q channels in the MWC first multiplies a sparse multiband signal $x(t)$ by a random periodic signal $p_i(t), i = 1, \ldots, q$, and then filters and samples product $x(t)p_i(t)$ at a sub-Nyquist rate (see Figure 1). The signals $p_i(t)$ are periodic extensions of distinct, finite-duration random square waves taking values $\{\pm 1\}$ that share a common period T_p seconds and chipping rate[1]. Here, we assume the chipping rate equals the Nyquist rate W and assume T_p is some integer multiple of the Nyquist period ($T_p = L/W, L > 1$). Each signal $p_i(t)$ has a Fourier series representation,

$$p_i(t) = \sum_{n=-\infty}^{\infty} P_i(n) e^{j\frac{2\pi}{T_p}nt},$$

where the $P_i(n)$'s are the Fourier series coefficients of $p_i(t)$. The impulse response of the filter is $h(t) = \frac{\pi W}{M}\text{sinc}(\frac{\pi W}{M}t)$ and thus has a cut-off frequency of $\omega_s/2$ radians per second, where $\omega_s = \frac{2\pi}{T_s} =$

[1]The chipping rate is defined as the fastest rate at which the signals can switch from $+1$ to -1 or vice versa.

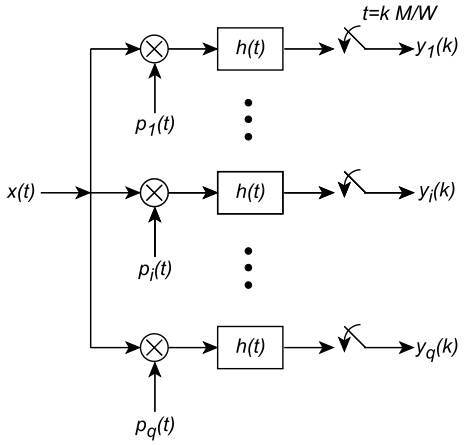

Figure 1: The modulated wideband converter [1].

$\frac{2\pi W}{M}$ is each channel's sampling rate. Every channel thus samples at a rate that is M times slower than the Nyquist rate and the system's average sampling rate is q/MW.

The modulated wideband converter and its associated recontruction algorithm address the situation where the exact number of occupied bands and their spectral locations are unknown. Complete signal reconstruction therefore entails the discovery of the number of occupied bands, their spectral locations, and their amplitudes from the sub-Nyquist samples $y_i(k),\ i = 1, \ldots, q$.

2 System Analysis

The following analysis offers a basic time and frequency domain description of the modulated wideband converter. We employ standard Fourier transform properties without explicit explanation for the sake of conciseness. The notational style is that of [5]. To denote Fourier transform pairs, we use the shorthand notation,

$$x(t) \xleftrightarrow{\text{FT}} X(j\omega),$$

and use the abbrevations FT and DTFT when referring to the Fourier transform and the discrete-time Fourier transform respectively.

Let $x(t)$ be a sparse multiband signal. Then by inspection of Figure 1 we have the following time and frequency domain relationships for the i^{th} channel, $i = 1, \ldots, q$.

Multiplication/Convolution:

$$x(t)p_i(t) \xleftrightarrow{\text{FT}} \sum_{m=-\infty}^{\infty} P_i(m)X(j\omega - jm\omega_p) \tag{1}$$

$$= \sum_{m=\lceil(\omega-\pi W)/\omega_p\rceil+1}^{\lfloor(\omega+\pi W)/\omega_p\rfloor} P_i(m)X(j\omega - jm\omega_p) \tag{2}$$

The summation limits are finite for a given ω because $x(t)$ is assumed bandlimited. The notation $\lceil\cdot\rceil$ and $\lfloor\cdot\rfloor$ denote the ceiling and floor rounding operations respectively, and $\omega_p = 2\pi W/L$ radians

per second.

Convolution (filtering)/Multiplication:

$$g_i(t) = x(t)p_i(t) * h(t) \xleftrightarrow{\text{FT}} G_i(j\omega) = \sum_{m=\lceil(\omega-\pi W)/\omega_p\rceil+1}^{\lfloor(\omega+\pi W)/\omega_p\rfloor} P_i(m)X(j\omega - jm\omega_p)H(j\omega) \tag{3}$$

$$= \sum_{m=-\lfloor\frac{1}{2\omega_p}(\omega_s+2\pi W)\rfloor+1}^{\lfloor\frac{1}{2\omega_p}(\omega_s+2\pi W)\rfloor} P_i(m)X(j\omega - jm\omega_p)\text{rect}(2\omega/\omega_s) \tag{4}$$

where $H(j\omega) = \text{rect}(2\omega_s/\omega)$ is the transfer function of an ideal low-pass filter with cut-off frequency $\omega_s/2$ and

$$\text{rect}(x) = \begin{cases} 1 & \text{for } -1 \le x \le 1 \\ 0 & \text{otherwise} \end{cases}.$$

Note that the low pass filter windows $X(j\omega)$ and its translates (i.e., restricts them to the interval $[-\omega_s/2, \omega_s/2]$) and hence removes the dependence on ω in the summation limits.

Sampling/Aliasing:

$$y_i(k) = g_i(kT_s) \tag{5}$$

$$\updownarrow \quad \text{DTFT};\omega_s$$

$$Y_i(e^{j\omega\frac{M}{W}}) = \frac{W}{M}\sum_{n=-\infty}^{\infty} G_i(j\omega + jn\omega_s) \tag{6}$$

$$= \frac{W}{M}\sum_{n=-\infty}^{\infty}\sum_{m=-\lfloor\frac{L}{2M}(M+1)\rfloor+1}^{\lfloor\frac{L}{2M}(M+1)\rfloor} P_i(m)X(j\omega - jm\omega_p + jn\omega_s)\text{rect}(2(\omega+n\omega_s)/\omega_s) \tag{7}$$

where (7) results from substituting (4) into (6) and the summation limits were rewritten using the definition of ω_p and ω_s. Because $Y_i(e^{j\omega\frac{M}{W}})$ is periodic with period $\omega_s = 2\pi W/M$, we can, without loss of information, restrict $Y_i(e^{j\omega\frac{M}{W}})$ to one period. This means we need only consider one term in the summation over n in (7). We choose to retain the $n = 0$ term and thus have the DTFT pair

$$Y_i(e^{j\omega\frac{M}{W}})\mathbf{1}_{[-\frac{\pi W}{M},\frac{\pi W}{M})} = \frac{W}{M}\sum_{m=-\lfloor\frac{L}{2M}(M+1)\rfloor+1}^{\lfloor\frac{L}{2M}(M+1)\rfloor} P_i(m)X(j\omega - jm\omega_p)\text{rect}(2\omega/\omega_s),$$

where $\mathbf{1}_{[\cdot)}$ denotes the indicator function. The Fourier series coefficients of $p_i(t)$ can now be directly computed,

$$\begin{aligned} P_i(m) &= \frac{1}{T_P}\int_0^{T_p} p_i(t)\, e^{-j\frac{2\pi}{T_p}mt}\, dt \\ &= \frac{1}{T_P}\sum_{l=0}^{L-1}\int_{l\frac{T_p}{L}}^{(l+1)\frac{T_p}{L}} p_{il}\, e^{-j\frac{2\pi}{T_p}mt}\, dt \\ &= \begin{cases} \sum_{l=0}^{L-1}\frac{p_{il}}{j2\pi m}\left(1 - e^{-j\frac{2\pi}{L}m}\right)e^{-j\frac{2\pi}{L}ml}, & m \neq 0 \\ \frac{1}{L}\sum_{l=0}^{L-1} p_{il}, & m = 0, \end{cases} \end{aligned}$$

where $p_{il} = p_i(t)$ for $t \in [lT_p/L, (l+1)T_p/L)$, to obtain

$$Y_i(e^{j\omega\frac{M}{W}})\mathbf{1}_{[-\frac{\pi W}{M},\frac{\pi W}{M})} = \frac{W}{M}\sum_{m=-\lfloor\frac{L}{2M}(M+1)\rfloor+1}^{\lfloor\frac{L}{2M}(M+1)\rfloor}\sum_{l=0}^{L-1} p_{il}\frac{1 - e^{-j\frac{2\pi}{L}m}}{j2\pi m}e^{-j\frac{2\pi}{L}ml}\text{rect}(\tfrac{M}{\pi W}\omega)X(j\omega - jm\tfrac{W}{L}),$$

for $i = 1, \ldots, q$, where this expression should be understood to be consistent with the expression for $P_i(0)$ given above.

We can express these q linear equations in matrix form

$$\mathbf{y}(\omega) = \mathbf{\Phi}\mathbf{\Psi}\mathbf{s}(\omega) \tag{8}$$

where

$$\begin{aligned}
y_i(\omega) &= Y_i(e^{j\omega\frac{M}{W}})\mathbf{1}_{[-\frac{\pi W}{M},\frac{\pi W}{M})} \\
\mathbf{\Phi}_{i,l} &= p_{il} \\
\mathbf{\Psi}_{l,m} &= \frac{M}{W}e^{-j\frac{2\pi}{L}lm} \\
s_m(\omega) &= \alpha_m \mathrm{rect}(\tfrac{M}{\pi W}\omega)\, X(j\omega - jm\tfrac{W}{L}) \\
\alpha_m &= \frac{1-e^{-j\frac{2\pi}{L}m}}{j2\pi m}, \quad \alpha_0 = 1/L,
\end{aligned}$$

for $i = 1,\ldots,q$, $l = 0,\ldots,L-1$, and $m = -\lfloor \frac{L}{2M}(M+1)\rfloor + 1,\ldots,\lfloor \frac{L}{2M}(M+1)\rfloor$. We emphasize that the elements of $\mathbf{y}(\omega)$ and $\mathbf{s}(\omega)$ are functions of ω over a specific interval—they are in fact spectral slices of $Y_i(e^{j\omega\frac{M}{W}})$ and $X(j\omega)$ respectively.

3 Support Recovery and Signal Reconstruction

Support recovery refers to the process of identifying which elements of $\mathbf{s}(\omega)$ contain the active bands that comprise $x(t)$. For the modulated wideband converter, support recovery proceeds similarly to the multi-coset recovery process [2,3] in that the covariance matrix of the output samples $y_i(k),\ i = 1,\ldots,q$, is examined. But unlike multi-coset support recovery, the modulated wideband converter does not use a modified MUSIC algorithm. It instead uses recent compressed sensing [6] ideas to recover the support of $\mathbf{s}(\omega)$. By definition, the covariance matrix $\mathbf{R}$ is related to the time-domain output samples,

$$\begin{aligned}
\mathbf{R}_{l,m} &\triangleq \int_{-\pi\frac{W}{M}}^{\pi\frac{W}{M}} y_l(\omega)y_m^*(\omega)\, d\omega && (9)\\
&= (M/W)^2 \int_{-\pi\frac{W}{M}}^{\pi\frac{W}{M}} Y_l(e^{j\omega\frac{M}{W}})Y_m^*(e^{j\omega\frac{M}{W}})(\omega)\, d\omega && (10)\\
&= 2\pi\frac{M}{W}\sum_{k=-\infty}^{\infty} y_l(k)y_m^*(k), && (11)
\end{aligned}$$

where $\mathbf{R}_{l,m}$ denotes the (l,m)th entry of $\mathbf{R}$ and (11) follows from the orthogonality property of the discrete-time Fourier transform. Note that to compute $\mathbf{R}$ exactly, one theoretically needs an infinite amount of data. In practice, we only have access to a finite amount of data $\mathbf{y}(k),\ k = 0,\ldots,N-1$, and the best we can do is estimate $\mathbf{R}$,

$$\widehat{\mathbf{R}}_{l,m} = 2\pi\frac{M}{W}\sum_{k=0}^{N-1} y_l(k)y_m^*(k). \tag{12}$$

The impact of using only a finite amount of data is beyond the scope of this report, but it does have an impact on the recoverability of the original signal.

In [7], Mishali and Eldar show that the support of $\mathbf{s}(\omega)$ can be recovered by solving an associated compressed sensing problem, namely, the sparse multiple measurement vector (MMV) problem. In MMV problems, the goal is to recover a set of jointly sparse vectors[2] from a set of incomplete measurements. To formulate this problem, we take an eigendecomposition of $\widehat{\mathbf{R}}$,

$$\begin{aligned}
\widehat{\mathbf{R}} &= \mathbf{U}^*\mathbf{\Lambda}\mathbf{U} && (13)\\
&= (\mathbf{U}^*\mathbf{\Lambda}^{1/2})((\mathbf{U}^*\mathbf{\Lambda}^{1/2}) && (14)\\
&= \mathbf{V}^*\mathbf{V}, && (15)
\end{aligned}$$

[2] A matrix X (composed of set of column vectors) is K *joint sparse* if there are at most K rows in X that contain nonzero elements.

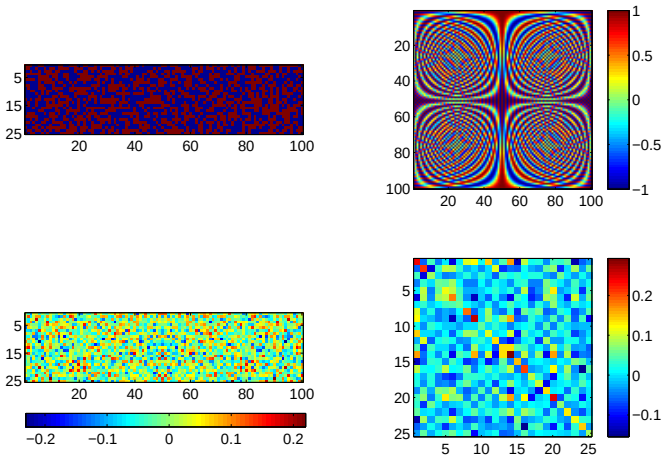

Figure 2: Graphical representation of the matrices (clockwise from the upper left-hand corner) $\mathbf{\Phi}, \mathbf{\Psi}, \mathbf{A} = \mathbf{\Phi\Psi}$, and $\widehat{\mathbf{R}}$.

and write down the linear system of equations,

$$\mathbf{V} = \mathbf{AS} \tag{16}$$

where $\mathbf{A} = \mathbf{\Phi\Psi}$ and $\mathbf{S}$ is an unknown matrix of size $M \times q$. The problem of solving for the unknown matrix $\mathbf{S}$ in (16) is called a multiple measurement vector problem because each column of $\mathbf{V}$ is thought of as an independent measurement of the cooresponding sparse columns of $\mathbf{S}$. Here, the important point is that the (joint) support of $\mathbf{S}$ equals the support of $\mathbf{s}(\omega)$. The proof of this claim is beyond the scope of this report, but details can be found in [7] and [1]. The solution to (8) is found by applying existing compressed sensing algorithms [7].

Once the support of $\mathbf{S}$ is found, we can reduce the dimension of $\mathbf{A}$ and invert (8) whereby recovering the active spectral slices, or in other words, recover all the information necessary to reconstruct the original analog signal $x(t)$. Let Ω denote the set of column indices that correspond to the recovered support. Collecting them into a matrix $\mathbf{A}_\Omega$, we can use its psuedoinverse $\mathbf{A}_\Omega^\dagger = \mathbf{A}_\Omega^*(\mathbf{A}_\Omega^*\mathbf{A}_\Omega)^{-1}\mathbf{A}_\Omega$ to invert (8),

$$\mathbf{s}_\Omega(t) = \mathbf{A}_\Omega^\dagger \mathbf{y}(t), \tag{17}$$

where $\mathbf{y}(t)$ and $\mathbf{s}_\Omega(t)$ are the inverse Fourier transforms of $\mathbf{y}(\omega)$ and $s_\Omega(\omega)$ respectively. To recover $x(t)$, we shift each component of $\mathbf{s}_\Omega(t)$ to their appropriate spectral locations:

$$x(t) = \sum_{l \in \Omega} s_{\Omega,l}(t) \exp\left(j2\pi \tfrac{W}{L} l t\right) \tag{18}$$

4 An Example

The MATLAB scripts accompanying this report, were used to simulate the sampling and reconstruction of a sparse multiband signal with three occupied bands, each having bandwidth 10 Hz, with an overall bandwidth of 1000 Hz ($K = 3$, $B = 10$ Hz, $W = 1000$ Hz, center frequencies of bands$= -152, 20, 350$ Hz). We simulated the input by generating a finite sequence of Nyquist samples $x(k/W)$ and then sub-sampled it using the modulated wideband converter over a simulated period of 20 seconds. The sampler had 25 channels, each of which sampled at 10 Hz ($q = 25$, $\frac{W}{M} = 10$ Hz). The overall simulated sampling rate was $\frac{qW}{M} = 250$ Hz, which is one quarter the Nyquist rate. Figures 2-4 show the results of the reconstruction. Figure 3 and 4 show that the band centre frequencies were successfully recovered. The errors in the reconstructed frequency response (Figure 3) and the time domain signal 4 are mainly due to the imperfect digital low pass filter used in the simulations. Figure 4 shows the real component of $x(t)$ was reconstructed with a mean-squared error 0.013.

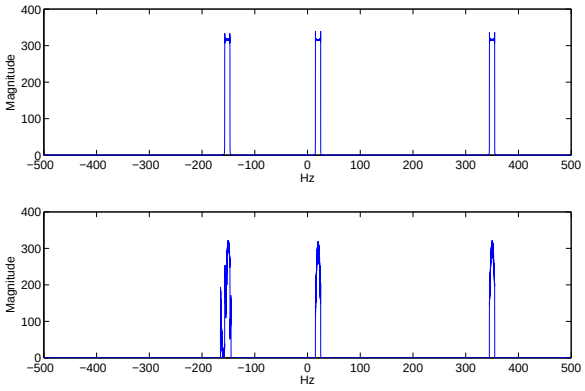

Figure 3: The plots show the frequency spectra of the original (top) and reconstructed (bottom) signals.

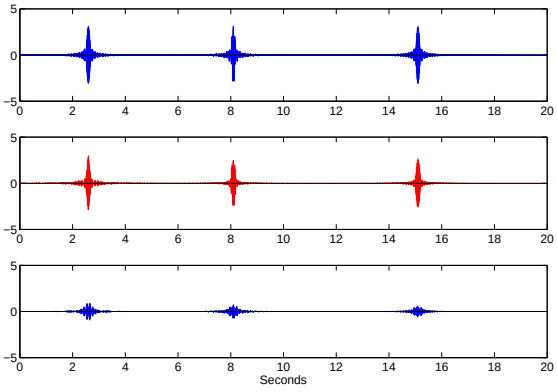

Figure 4: The top and middle panels show the original (blue) and reconstructed (red) signals, respectively. The bottom panel displays the difference signal. The original signal is shifted to match the delayed output of the system. The delay is caused by the low pass filter. The signals are of length $20,000$.

References

[1] M. Mishali and Y.C. Eldar, "From theory to practice: Sub-nyquist sampling of sparse wideband analog signals," *Selected Topics in Signal Processing, IEEE Journal of*, vol. 4, no. 2, pp. 375 –391, Apr 2010.

[2] P. Feng and Y. Bresler, "Spectrum-blind minimum-rate sampling and reconstruction of multiband signals," *Proc. IEEE International Conf. on Acoustics, Speech, and Signal Processing*, vol. 3, pp. 1688–1691, May 1996.

[3] Ping Feng, *Universal Minimum-Rate Sampling and Spectrum-Blind Reconstruction for Multiband Signals*, Ph.d., University of Illinois at Urbana-Champaign, Urbana-Champaign, IL U.S.A., 1997.

[4] J.A. Tropp, J.N. Laska, M.F. Duarte, J.K. Romberg, and R.G. Baraniuk, "Beyond Nyquist: Efficient sampling of sparse bandlimited signals," *IEEE Trans. Info. Th.*, vol. 56, no. 1, pp. 520–544, Jan 2010.

[5] Richard Roberts and Clifford Mullis, *Digital Signal Processing*, Addison-Wesley Publishing Co., Inc., 1987.

[6] E.J. Candes and M.B. Wakin, "An introduction to compressive sampling," *IEEE Signal Processing Mag.*, vol. 25, no. 2, pp. 21–30, Mar 2008.

[7] M. Mishali and Y.C. Eldar, "Reduce and boost: Recovering arbitrary sets of jointly sparse vectors," *IEEE Trans. Signal Processing*, vol. 56, no. 10, pp. 4652–4702, Oct 2008.